Subset Selection Based RIS-Aided Beamforming for Joint Radar-Communications

Evangelos Vlachos[1] and Aryan Kaushik[2]
[1]Industrial Systems Institute (ISI), ATHENA R&I Center, Greece
[2]School of Engineering and Informatics, University of Sussex, UK
Emails: evlachos@athenarc.gr, aryan.kaushik@sussex.ac.uk

2023 IEEE Wireless Communications and Networking Conference (WCNC) | 978-1-6654-9122-8/23/$31.00 ©2023 IEEE | DOI: 10.1109/WCNC55385.2023.10119089

***Abstract*—Joint radar-communications (JRC) benefits from multi-functionality of radar and communication operations using same hardware and radio frequency (RF) spectrum resources. Thus, JRC systems possess very high potential to be employed into the sixth generation (6G) standards. Besides, intelligent reflecting surfaces have attracted wide attention in communication systems, due to low complexity of implementation. This paper designs a dynamic beamformer for reconfigurable intelligent surfaces (RIS) which maximizes spectral efficiency (SE). We jointly express the mutual information rate for communication and radar entities including a weighting factor which depicts the dominance of one operation over the other. The joint-SE based proposed method optimally selects the RIS subset. Furthermore, when the communication operation takes place the proposed method takes into account the interference occurring from the radar operation and vice-versa. Fractional programming based selection procedure is used for solving the problem of subset selection. Simulation results are presented and compared with different baselines to show effectiveness of the proposed method.**

***Index Terms*—Joint radar-communications, flexible beamforming, RF selection, interference, hybrid precoder.**

I. Introduction

Mobile connectivity is expected to be over 70% of the global population, and fifth generation (5G) connections are estimated to constitute towards 1.4 billion mobile devices by 2023 [1]. By 2027, 5G subscriptions will be 4.4 billion presenting faster growth than previous generation standards, and average monthly usage per smartphone reaching to 40 GB globally, and 52 GB of data traffic in both Western Europe and North America [2]. Thus to initiate the implementation of sixth generation (6G) wireless standards, more advanced technical solutions such as sharing of hardware and spectral resources for several wireless applications, are required to make efficient use of the available resources. This will lead to decongestion of existing sub 6-GHz spectrum which implements majority of the current mobile services, and solve hardware inefficiency issues with massive connectivity.

One such approach is to unify sensing and communications operations on a single hardware and use of same spectral resources, where sensing collects and extracts information, such as target detection, and using radio waves for tracking movement, while communication possesses transfer of information [3]–[5]. The emerging joint radar and communications (JRC) systems accommodate multiple functionalities of these operations, massive connectivity with limited resources, and provide wide applications in future wireless, defence, aerial, vehicular, internet-of-things and space [4]–[7]. To achieve high beamforming gains with high degrees of freedom, JRC can employ multiple-input multiple-output (MIMO) antennas which improves range resolution and also makes up for the high path loss associated with high-frequency bands such as millimeter wave [8], [9].

Hybrid precoding architecture, which constitutes of analog and digital precoding, has been implemented for 5G MIMO systems to obtain energy and hardware efficient designs such as in [10]–[12]. Recently, hybrid precoding has been implemented in energy and hardware efficient JRC [13] and it is also implemented with low resolution sampling based digital-to-analog converters (DACs) in JRC [14]. Advanced multiple access approaches such as the non-orthogonal multiple access (NOMA) and rate splitting multiple access (RSMA) have also been incorporated with JRC [15], [16] for interference management and massive connectivity. Further advanced signal processing approaches in JRC implement low complexity waveform designs and index modulation based JRC with antenna and frequency agility [17]–[19]. However, latest JRC systems do not consider jointly designing rate for both the operations with flexible beamforming while taking into account the interference occurring from each of the operations in dual function JRC.

Besides, intelligent reflecting surfaces have attracted wide attention in communication systems, due to their low complexity and higher energy efficiency. Reconfigurable intelligent surfaces (RIS) leverage smart radio surfaces with high number of small antennas or metamaterial elements based on a programmable structure that can be used to control the propagation of electromagnetic waves [20], [21]. RIS configurations can be realized by incorporating large number of antenna elements with reconfigurable processing networks which provides a continuous antenna aperture. Furthermore, the use of intelligent surfaces has started to receive attention in radar systems such as in [22]–[24]. However, JRC systems are not widely studied with RIS-aided beamforming and hardware efficient approaches. Furthermore, latest JRC systems do not consider jointly designing rate for both the operations with flexible RIS-aided beamforming such as subset selection based approach while taking into account the interference occurring from each of the operations in dual function JRC.

978-1-6654-9122-8/23/$31.00 ©2023 IEEE

Contributions: In this paper, for 6G JRC systems, we jointly design radar-communication rate in terms of weighting formulation which decides the dominance of one operation over the other while both radar and communication operations take place simultaneously. We employ this formulation to solve an interference-oriented spectral efficiency (SE) maximization problem while interference minimization takes place and power constraints are imposed on both the operations. We develop a selection procedure based on fractional programming which is employed to optimize the number of available RF chains in dual function RIS-aided JRC system while interference is minimized and joint-SE is maximized. This procedure leads to highly spectral efficient design with low hardware complexity (via RF chain selection). Such framework carries high potential to be used in the future 6G wireless communication standards. Numerical results show communication and radar performance gains of joint SE-based proposed approach over baselines for different weighting factor values and interference scenarios.

Notation: The notation $\mathbf{M}$ represents matrix, $\mathbf{m}$ represents vector, m is scalar entity, tr(.) and $|.|$ represent trace and determinant functions, $(.)^{\mathrm{T}}$ denotes transpose, $(.)^{\mathrm{H}}$, $\|.\|_F$ and $\|.\|_2$ represent complex conjugate transpose, Frobenius norm, and Euclidean norm, respectively. The notation $[\mathbf{M}]_{m:k}$ is the submatrix with the m-th to k-th columns of $\mathbf{M}$ and $\mathbf{m}_m$ is m-th element of $\mathbf{m}$; $\mathbf{I}$ is the identity matrix. $\mathbb{C}$ and $\mathbb{R}$ represent sets of complex and real numbers, respectively, and $\mathcal{E}$ denotes expectation operator.

II. System and Channel Models

The considered system is composed of N-element reconfigurable intelligent surface (RIS) which assists the downlink communication between a base-station and a user (UE)/receiver, as shown in Fig. 1. The RIS implements a dual function JRC with hybrid beamforming which employs baseband precoding and analog precoding.

The source signal from the RIS constitutes $\mathbf{s} = \begin{bmatrix} \mathbf{s}_{\mathrm{C}}^{\mathrm{T}} & \mathbf{s}_{\mathrm{R}}^{\mathrm{T}} \end{bmatrix}^{\mathrm{T}}$, where $\mathbf{s}_{\mathrm{C}} \in \mathbb{C}^{\frac{N}{2}\times 1}$ refers to the communication vector term and $\mathbf{s}_{\mathrm{R}} \in \mathbb{C}^{\frac{N}{2}\times 1}$ is for the radar operation. Then, the transmitted signal from the RIS is:

$$\mathbf{x} = \begin{bmatrix} \mathbf{s}_{\mathrm{C}}^{\mathrm{T}}\mathbf{\Phi}_{\mathrm{C}} & \mathbf{s}_{\mathrm{R}}^{\mathrm{T}}\mathbf{\Phi}_{\mathrm{R}} \end{bmatrix}^{\mathrm{T}} \tag{1}$$

where $\mathbf{\Phi}_{\mathrm{C}}^{\frac{N}{2}\times\frac{N}{2}}$ and $\mathbf{\Phi}_{\mathrm{R}}^{\frac{N}{2}\times\frac{N}{2}}$ are the diagonal matrices with the complex reflection (constant modulus elements) of the RIS for the communications and radar operations, respectively.

Following that, we describe the general channel model that can be used for both communication and radar operations. For N_c multipaths, the baseband channel matrix is represented as

$$\mathbf{H} = \frac{N}{\sqrt{N_{\mathrm{c}}}} \sum_{l=1}^{N_{\mathrm{c}}} \alpha_l \mathbf{a}_{\mathrm{R}}(\phi_l^r)\mathbf{a}_{\mathrm{T}}^{\mathrm{H}}(\phi_l^t), \tag{2}$$

with α_l being the channel gain of l-th path, and N_{c} being the number of clustered multipaths. The term $\mathbf{a}_{\mathrm{T}}(\phi_l^t) = \frac{1}{\sqrt{N}}[1, e^{j\frac{2\pi}{\lambda}d\sin(\phi_l^t)}, ..., e^{j(N-1)\frac{2\pi}{\lambda}d\sin(\phi_l^t)}]^T$ represents the steering vector for transmission. The departure angle is represented as ϕ_l^t with d being spacing between antennas and λ being wavelength. Similarly, the term $\mathbf{a}_{\mathrm{R}}(\phi_l^r)$ represents array response vector for receiver. The angle of arrival is represented as ϕ_l^r. It is assumed that the channel state information (CSI) of communication channel is known at transmitter.

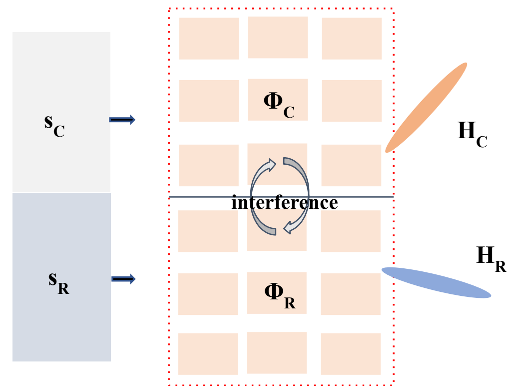

Fig. 1: Joint Radar and Communication RIS.

III. Mutual Information for JRC-RIS

In this section we present mutual information expressions for the dual function JRC system model where we consider two of the possible cases: (i) with no impact of interference of one operation over the other operation which presents an idealized case, and (ii) while taking into account the impact of interference of one operation over the other operation. The communication spectral efficiency is well known in literature.

In terms of the literature surrounding radar mutual information, reference [27] describes waveform design approach while taking into account radar mutual information between target reflections and target responses. Furthermore, the main purpose of the radar mutual information is to evaluate the radar performance, such as in [28], [29] mutual information is described between target impulse response and echo/reflected signal, provided there is prior knowledge of the dual function JRC transmit signal or radar-only transmit signal. JRC systems such as in [30], express the radar mutual information between the signal and target impulse response of radar and communication signals, while assuming that both radar and communication signals partly have common information on the target.

Let us first consider the idealized case where the two systems have dedicated separate hardware that do not interfere with each other. The mutual information (MUI) can be expressed as [31]:

$$I^{\mathrm{opt}} = \log_2(1+\frac{1}{\sigma_n^2}\|\mathbf{H}_{\mathrm{C}}\mathbf{\Phi}_{\mathrm{C}}\|_F^2)+\log_2(1+\frac{1}{\sigma_n^2}\|\mathbf{H}_{\mathrm{R}}\mathbf{\Phi}_{\mathrm{R}}\|_F^2), \tag{3}$$

where $\mathbf{H}_{\mathrm{C}}$, $\mathbf{H}_{\mathrm{R}}$ are the channel matrices for the communications and radar, respectively. For the RIS beamforming diagonal matrices we have that $\|\mathbf{\Phi}_{\mathrm{C}}\|^2 = \|\mathbf{\Phi}_{\mathrm{R}}\|^2 = P_{\max}/2$. The term σ_n^2 accounts for the AWGN variance.

Considering the interference terms between the communications and radar subsystems, the MUI can be expressed as:

$$I^{\text{int}} = \log_2(1 + \frac{1}{\sigma_n^2 + \sigma_{\text{R}}^2}\|\mathbf{H}\mathbf{\Phi}_{\text{C}}\|_F^2 + \log_2(1 + \frac{1}{\sigma_n^2 + \sigma_{\text{C}}^2}\|\mathbf{H}\mathbf{\Phi}_{\text{R}}\|_F^2) \leq I^{\text{opt}}, \tag{4}$$

where σ_{R}^2 corresponds to the radar interference while communication operation is taking place in the dual function JRC system, and similarly σ_{C}^2 corresponds to the communication interference to the radar operation, with $\sigma_{\text{R}}^2 = \|\mathbf{H}_{\text{R}}\mathbf{\Phi}_{\text{C}}\|^2$ and $\sigma_{\text{C}}^2 = \|\mathbf{H}_{\text{C}}\mathbf{\Phi}_{\text{R}}\|^2$, respectively.

Previously, it has been proposed a weighted MUI metric that utilizes a weighting factor $\rho \in [0, 1]$ for the MUI of each subsystem. For the case of MUI with interference we have:

$$I^{\text{w}} = 2\rho \log_2(1 + \frac{1}{\sigma_n^2 + \sigma_{\text{R}}^2}\mathbf{H}\mathbf{\Phi}_{\text{C}}\|_F^2) + 2(1-\rho)\log_2(1 + \frac{1}{\sigma_n^2 + \sigma_{\text{C}}^2}\mathbf{H}\mathbf{\Phi}_{\text{R}}\|_F^2). \tag{5}$$

Note that the JRC weighting term ρ describes the dominance of one operation over the other, depending on its value between 0 and 1, i.e., $\rho \in [0, 1]$. For instance, when ρ value is high, JRC system prioritizes communication operation and when ρ value is low, JRC system prioritizes radar sensing operation. For $\rho = \frac{1}{2}$, it represents that both the operations have same weighting in dual function JRC system.

IV. RIS Subset Selection

In this section, we propose a mathematical modeling for the dynamic reconfiguration of the RIS for JRC operation. We consider that the diagonal matrices $\mathbf{\Phi}_{\text{C}}$ and $\mathbf{\Phi}_{\text{R}}$ take values from the columns of the discrete Fourier Transform matrix, $\mathbf{F}_{\text{RF}} = e^{-j2\pi\mathbf{E}}$ with $\mathbf{E} = [0, 1, \ldots, N/2-1]^{\text{T}}[0, 1, \ldots, N/2-1]/(N/2)$. These matrices represent the complex configuration of the communication and radar parts of the RIS, respectively. In case of a static configuration, where the RIS reflection matrices are based on the k-th column of $\mathbf{F}_{\text{RF}}$, and the m-th column for the radar, we would have:

$$\mathbf{\Phi}_{\text{C}} = \text{diag}([\mathbf{F}_{\text{RF}}]_k), \text{ and } \mathbf{\Phi}_{\text{R}} = \text{diag}([\mathbf{F}_{\text{RF}}]_m). \tag{6}$$

Proposition 1. *To introduce a dynamic reconfiguration model, let us define two diagonal and binary matrices,* $\mathbf{D}_R \in \{0,1\}^{\rho N \times \rho N}$ *and* $\mathbf{D}_C \in \{0,1\}^{(1-\rho)N \times (1-\rho)N}$ *with* $tr(\mathbf{D}_C) = tr(\mathbf{D}_R) = 1$*. Then, the RIS beamformer for each operation can be expressed as:*

$$\mathbf{\Phi}_C = diag(\mathbf{F}_{RF}\mathbf{D}_C\mathbf{e}_{\rho N}), \text{ and } \mathbf{\Phi}_R = diag(\mathbf{F}_{RF}\mathbf{D}_R\mathbf{e}_{(1-\rho)N}),$$

where $\mathbf{e}_{\rho N}$ *is a* $2\rho N \times 1$ *vector with ones, and respectively for* $\mathbf{e}_{(1-\rho)N}$*.*

As it will become clear later, the definition of the binary matrices $\mathbf{D}_{\text{R}}$ and $\mathbf{D}_{\text{C}}$ enables the utilization of subset selection optimization techniques. Recall from the previous section, that the MUI for the communications and radar operations was determined by the weighting factor ρ. This weighting can be seen as dynamic resource allocation for the RIS beamformer, e.g., ρ% of $\mathbf{\Phi}$ columns can be used for communications and the rest $(1-\rho)$% for radar. Using Proposition 1, this weighting is represented by the dimension of the diagonal matrices $\mathbf{D}_{\text{R}}$ and $\mathbf{D}_{\text{C}}$.

The problem of RIS design for maximizing the weighted mutual information I^{w} is expressed as follows:

$$\begin{aligned} \max_{\mathbf{\Phi}_{\text{R}}, \mathbf{\Phi}_{\text{C}}} \; & 2\rho \log_2(1 + \frac{\sigma_s^2}{\sigma_n^2 + \sigma_{\text{R}}^2}\|\mathbf{H}\mathbf{\Phi}_{\text{C}}\|_F^2 \\ & + 2(1-\rho)\log_2(1 + \frac{\sigma_s^2}{\sigma_n^2 + \sigma_{\text{C}}^2}\|\mathbf{H}\mathbf{\Phi}_{\text{R}}\|_F^2), \\ \text{subject to } & 2\rho\|\mathbf{\Phi}_{\text{C}}\|^2 + 2(1-\rho)\|\mathbf{\Phi}_{\text{R}}\|^2 = P_{\max}, \end{aligned} \tag{7}$$

where $P_{\max}$ is the maximum available energy for the transmission of both communication and radar operation.

Using Proposition 1, it can be shown that (c.f., Appendix), the mutual information maximization problem (7) becomes,

$$\begin{aligned} \max_{\mathbf{D}_{\text{C}}, \mathbf{D}_{\text{R}}} \; & \log_2(1 + \frac{1}{\sigma_n^2 + \|\mathbf{H}_{\text{R}}\text{diag}(\mathbf{F}_{\text{RF}}\mathbf{D}_{\text{C}})\|_F^2}\|\mathbf{H}\text{diag}(\mathbf{F}_{\text{RF}}\mathbf{D}_{\text{C}})\|_F^2 \\ & + \frac{1}{\sigma_n^2 + \|\mathbf{H}_{\text{C}}\text{diag}(\mathbf{F}_{\text{RF}}\mathbf{D}_{\text{R}})\|_F^2}\|\mathbf{H}\text{diag}(\mathbf{F}_{\text{RF}}\mathbf{D}_{\text{R}})\|_F^2), \\ \text{subject to } & \mathbf{D}_{\text{C}}, \mathbf{D}_{\text{R}} \in \{0, 1\}. \end{aligned} \tag{8}$$

To solve (8) we proceed with a series of approximations which will render the problem to a convex one.

Assuming that the JRC system operates at *high noise regime*, the second part of the logarithms go to zero, thus, using the first order Taylor expansion for the logarithm, $\log(1+x) \approx x$ for $x \to 0$, we have that:

$$\begin{aligned} & \log_2(1 + \frac{1}{\sigma_n^2 + \|\text{diag}(\mathbf{F}_{\text{RF}}\mathbf{D}_{\text{C}})^{\text{H}}\mathbf{H}_{\text{R}}\|^2}\|\text{diag}(\mathbf{F}_{\text{RF}}\mathbf{D}_{\text{C}})^{\text{H}}\mathbf{H}\|^2 \\ & \quad + \frac{1}{\sigma_n^2 + \|\text{diag}(\mathbf{F}_{\text{RF}}\mathbf{D}_{\text{R}})^{\text{H}}\mathbf{H}_{\text{C}}\|^2}\|\text{diag}(\mathbf{F}_{\text{RF}}\mathbf{D}_{\text{R}})^{\text{H}}\mathbf{H}\|^2) \\ & \approx \frac{1}{\sigma_n^2 + \|\text{diag}(\mathbf{F}_{\text{RF}}\mathbf{D}_{\text{C}})^{\text{H}}\mathbf{H}_{\text{R}}\|^2}\|\text{diag}(\mathbf{F}_{\text{RF}}\mathbf{D}_{\text{C}})^{\text{H}}\mathbf{H}\|^2 \\ & \quad + \frac{1}{\sigma_n^2 + \|\text{diag}(\mathbf{F}_{\text{RF}}\mathbf{D}_{\text{R}})^{\text{H}}\mathbf{H}_{\text{C}}\|^2}\|\text{diag}(\mathbf{F}_{\text{RF}}\mathbf{D}_{\text{R}})^{\text{H}}\mathbf{H}\|^2. \end{aligned} \tag{9}$$

Next, the requirement for binary entries for the selection matrices is relaxed to box constraint, i.e., $[\mathbf{D}_{\text{C}}]_{n,n}, [\mathbf{D}_{\text{R}}]_{n,n} \in (0, 1)$. Then, the problem (7) can be written as:

$$\begin{aligned} \max_{\mathbf{D}_{\text{C}}, \mathbf{D}_{\text{R}}} \; & \frac{1}{\sigma_n^2 + \|\text{diag}(\mathbf{F}\mathbf{D}_{\text{C}})^{\text{H}}\mathbf{H}_{\text{R}}\|^2}\|\text{diag}(\mathbf{F}_{\text{RF}}\mathbf{D}_{\text{C}})^{\text{H}}\mathbf{H}\|^2 \\ & + \frac{1}{\sigma_n^2 + \|\text{diag}(\mathbf{F}_{\text{RF}}\mathbf{D}_{\text{R}})^{\text{H}}\mathbf{H}_{\text{C}}\|^2}\|\text{diag}(\mathbf{F}_{\text{RF}}\mathbf{D}_{\text{R}})^{\text{H}}\mathbf{H}\|^2 \\ \text{subject to } & [\mathbf{D}_{\text{C}}]_{n,n}, [\mathbf{D}_{\text{R}}]_{n,n} \in (0, 1). \end{aligned} \tag{10}$$

We apply the Dinkelbach approximation to the fractional problem in (10), deriving the following linear approximation:

$$\begin{aligned} \max_{\mathbf{D}_{\text{C}}, \mathbf{D}_{\text{R}}} \; & \|\text{diag}(\mathbf{F}_{\text{RF}}\mathbf{D}_{\text{C}})^{\text{H}}\mathbf{H}\|^2 + \|\text{diag}(\mathbf{F}_{\text{RF}}\mathbf{D}_{\text{R}})^{\text{H}}\mathbf{H}\|^2 \\ & - \kappa_{\text{C}}(\sigma_n^2 + \|\text{diag}(\mathbf{F}_{\text{RF}}\mathbf{D}_{\text{C}})^{\text{H}}\mathbf{H}_{\text{R}}\|^2) \\ & - \kappa_{\text{R}}(\sigma_n^2 + \|\text{diag}(\mathbf{F}_{\text{RF}}\mathbf{D}_{\text{R}})^{\text{H}}\mathbf{H}_{\text{C}}\|^2), \\ \text{subject to } & [\mathbf{D}_{\text{C}}]_{n,n}, [\mathbf{D}_{\text{R}}]_{n,n} \in (0, 1). \end{aligned} \tag{11}$$

Algorithm 1 Subset Selection Method

Input: $\mathbf{R}$, $\mathbf{R}_{\mathrm{C}}$, $\mathbf{R}_{\mathrm{R}}$, ρ
Output: Diagonal binary matrices $\mathbf{D}_{\mathrm{C}}$ and $\mathbf{D}_{\mathrm{R}}$

Initialize $\kappa_{\mathrm{C}}^{(0)} = \kappa_{\mathrm{R}}^{(0)} = 1$, $\mathbf{F}_{\mathrm{RF}} = e^{-j2\pi\mathbf{E}}$ with $\mathbf{E} = [0, 1, \ldots, N/2-1]^{\mathrm{T}}[0, 1, \ldots, N/2-1]/(N/2)$.
for $i = 1, 2, \ldots, I_{\max}$ **do**
  $c_{\mathrm{C}}^{(i)} = \|\mathrm{diag}(\mathbf{F}_{\mathrm{RF}}\mathbf{D}_{\mathrm{C}}^{(i)})^{\mathrm{H}}\mathbf{H}\|^2$
  $c_{\mathrm{R}}^{(i)} = \|\mathrm{diag}(\mathbf{F}_{\mathrm{RF}}\mathbf{D}_{\mathrm{R}}^{(i)})^{\mathrm{H}}\mathbf{H}\|^2$
  $\eta_{\mathrm{C}}^{(i)} = \sigma_n^2 + \|\mathrm{diag}(\mathbf{F}_{\mathrm{RF}}\mathbf{D}_{\mathrm{C}})^{\mathrm{H}}\mathbf{H}_{\mathrm{R}}\|^2$
  $\eta_{\mathrm{R}}^{(i)} = \sigma_n^2 + \|\mathrm{diag}(\mathbf{F}_{\mathrm{RF}}\mathbf{D}_{\mathrm{R}})^{\mathrm{H}}\mathbf{H}_{\mathrm{C}}\|^2$
  $\max_{\tilde{\mathbf{D}}_{\mathrm{C}}} c_{\mathrm{C}}^{(i)} - \kappa_{\mathrm{C}}^{(i-1)}\eta_{\mathrm{C}}^{(i)}$ s.t. $[\mathbf{D}_{\mathrm{C}}]_{n,n} \in (0,1)$
  $\mathbf{D}_{\mathrm{C}} = \mathrm{thres}_{\rho}(\tilde{\mathbf{D}}_{\mathrm{C}})$
  $\max_{\tilde{\mathbf{D}}_{\mathrm{R}}} c_{\mathrm{R}}^{(i)} - \kappa_{\mathrm{R}}^{(i-1)}\eta_{\mathrm{R}}^{(i)}$ s.t. $[\mathbf{D}_{\mathrm{R}}]_{n,n} \in (0,1)$
  $\mathbf{D}_{\mathrm{R}} = \mathrm{thres}_{\rho}(\tilde{\mathbf{D}}_{\mathrm{R}})$
  $\kappa_{\mathrm{C}}^{(i)} = \frac{c_{\mathrm{C}}^{(i)}}{\eta_{\mathrm{C}}^{(i)}}$ and $\kappa_{\mathrm{R}}^{(i)} = \frac{c_{\mathrm{R}}^{(i)}}{\eta_{\mathrm{R}}^{(i)}}$
end for

Thus, we end up with the convex problem in (11), which is an approximation for (7), and can be solved using any available interior-point method (e.g., CVX [26]).

The overall algorithm is summarized in 1, which requires the covariance matrices for the communications and radar channels. The output are the diagonal matrices that maximize the mutual information in (7). Note that, we use the function $\mathrm{thres}(\cdot)_{\rho}$, which performs thresholding on the values of its input matrix. The parameter ρ determines the thresholding lower bound for the matrices $\tilde{\mathbf{D}}_{\mathrm{C}}$ and $\tilde{\mathbf{D}}_{\mathrm{R}}$. Next, we present the numerical results to show the significance of our proposed method.

V. Simulation Results

We evaluate the performance of the proposed approach to ensure the effectiveness of the proposed method. For evaluation of the proposed technique, we compare with the following baselines:

- *No interference* case, which represents the optimal upper bound for the weighted MUI.
- *With interference* case, which represents the lower bound for the weighted MUI, assuming that no measure is taken for interference mitigation.
- *Hybrid Beamforming* is also an idealized case where fully connected hybrid beamforming is performed instead of RIS, with perfect channel knowledge for both communications and radar.
- *Static RIS configuration* represents a static beamforming technique, where the RIS reflection matrices are randomly chosen from the DFT matrix $\mathbf{F}_{\mathrm{RF}}$.

In the following results, for simplicity, we assume that we have the same number of users and targets, and their placement is equispaced and alternatively.

Let us first depict the results for the MUI over the signal-to-noise ratio (SNR), which is defined as $\mathrm{SNR} = \frac{1}{\sigma_n^2}$. In Fig. 2, we show the MUI for the case of $\rho = 1$. Recall that, the weighting between the two MUI terms is a parameter that is being defined by the user, depending on needs of the application. Note that, for the two extreme cases, where $\rho = 1$ or $\rho = 0$, there is no interference, thus all techniques are expected to behave similarly. The proposed technique follows closely the other baselines, given that does not requires the instantaneous channel matrices, thus, lags some performance at the higher SNR regime.

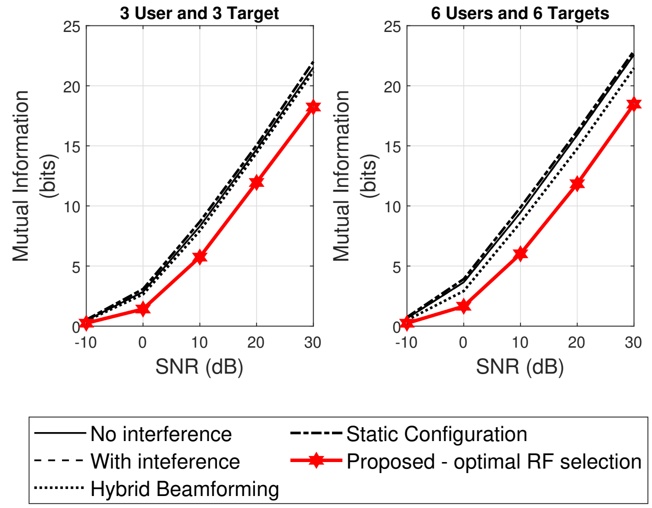

Fig. 2: Mutual information performance versus SNR for different target and user scenarios, $N = 32, \rho = 1$.

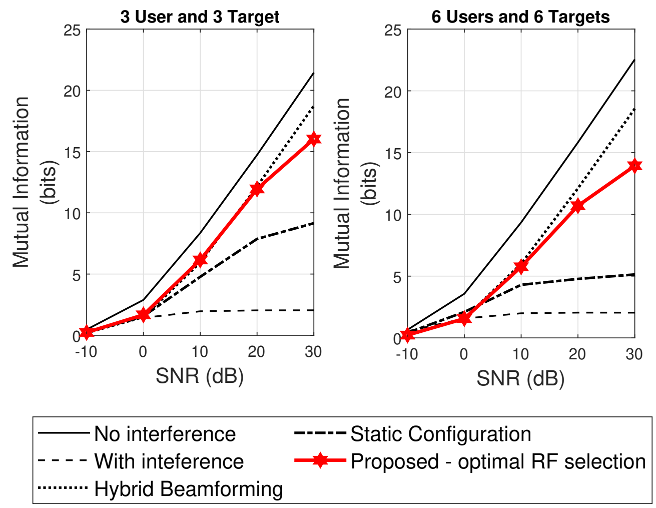

Fig. 3: Mutual information performance versus SNR for different target and user scenarios, $N = 32, \rho = 0.5$.

In Fig. 6 we show the results for the MUI over the number of the antennas N, for the case of 6 users and 6 targets. As the antenna size, and thus, the angle resolution, increases, the performance of all techniques is improved. It is important to stress out that the proposed technique has significant benefits from larger antenna arrays.

Next, we evaluate the radar performance, in terms of Nor-

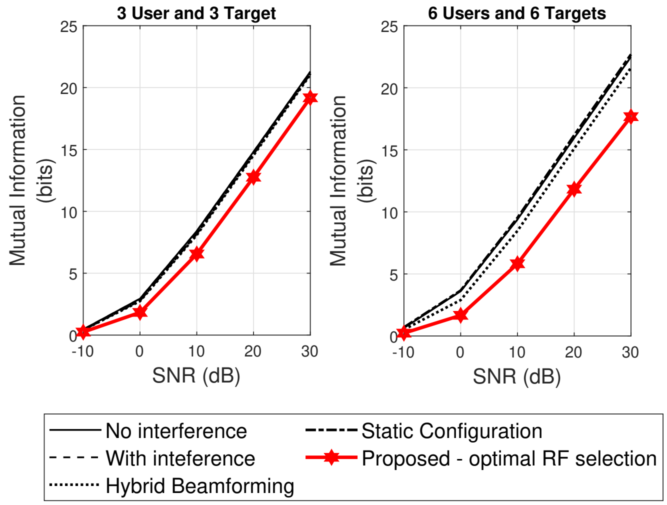

Fig. 4: Mutual information performance versus SNR for different target and user scenarios, $N = 32, \rho = 0$.

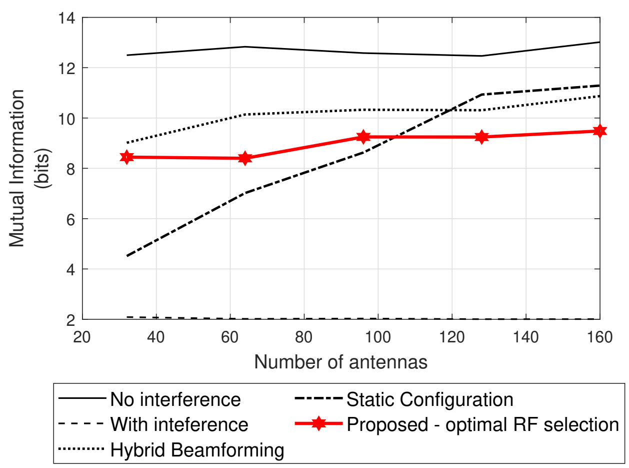

Fig. 5: Mutual information performance versus number of transmit antennas at $\mathrm{SNR} = 15\mathrm{dB}, \rho = 0.5$. The number of targets is 3.

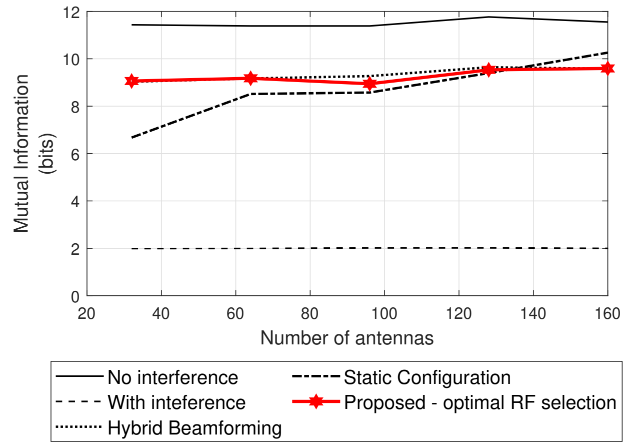

Fig. 6: Mutual information performance versus number of transmit antennas at $\mathrm{SNR} = 15\mathrm{dB}, \rho = 0.5$. The number of targets is 1.

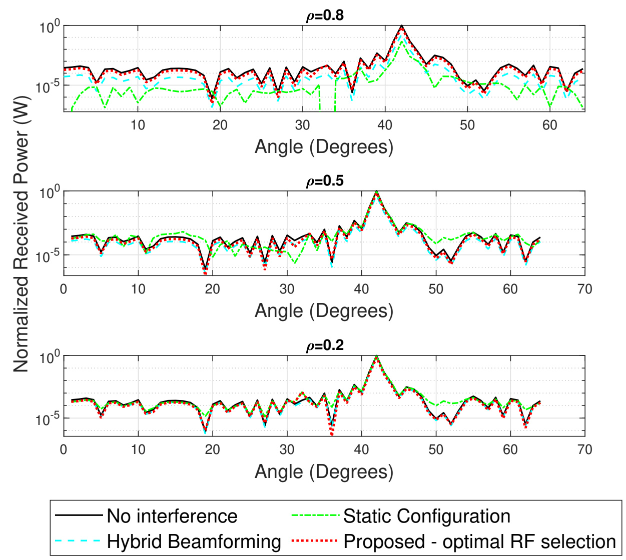

Fig. 7: Normalized received power performance, $N = 64, \mathrm{SNR} = 5\mathrm{dB}$. The number of targets is 1.

malized Received Power (NRP), defined as:

$$\mathrm{NRP} = \|\mathbf{H}_{\mathrm{R}}\mathbf{\Phi}_{\mathrm{R}}\|_F^2. \tag{12}$$

In Fig. 7, we show the beampattern for three cases of ρ. The radar channels have been constructed assuming that there is 1 target placed at angle 42 degrees. All the techniques are able to detect the the angle of the obstacle with acceptable performance. However, for $\rho = 0.8$, which benefits the communication operation, the static configuration has lower received power. The proposed technique exhibits close to the optimal performance (no interference and hybrid beamforming cases). In Fig. 8, we evaluate the performance of the techniques when the number of the targets is 2.

VI. Conclusion

This paper designs joint SE maximization problem for RIS-aided precoding based MIMO JRC systems with dual function radar and communication operations. We consider interference from one operation to the other in our problem formulation, and implement an optimal RF chain subset selection procedure for flexible RIS-aided beamforming design. The proposed method based on fractional programming yields good joint rate performance when compared with existing baselines which implement fixed number of RF chains and different interference cases. The effect of weighting factor which prioritizes one operation over the other, has also been observed via numerical results and comparison with baselines.

VII. Appendix

In this section, we prove the equivalence of the expressions of the standard weighted MUI in (5) and the proposed one in (8), where the weighting factor ρ has been incorporated in the

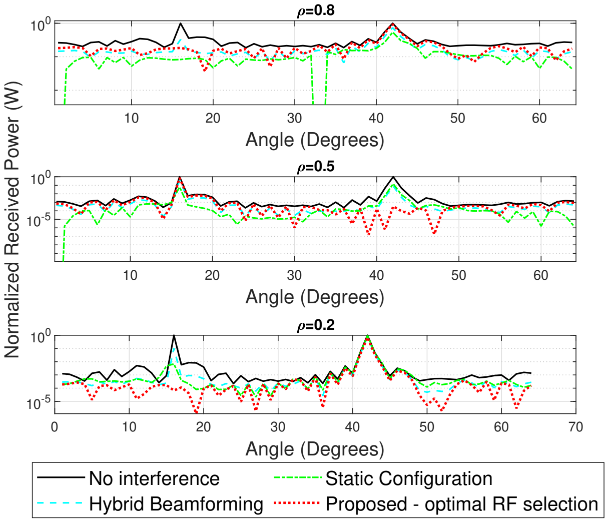

Fig. 8: Normalized received power performance, $N = 64, \mathrm{SNR} = 5\mathrm{dB}$. The number of targets is 2.

binary matrices. Let us rewrite the proposed expression for the MUI from (8):

$$\log_2(1 + \frac{1}{\sigma_n^2 + \sigma_{\mathrm{R}}^2}\|\mathbf{H}\mathrm{diag}(\mathbf{F}_{\mathrm{RF}}\mathbf{D}_{\mathrm{C}}\mathbf{e}_{\rho N})\|_F^2 + \log_2(1 + \frac{1}{\sigma_n^2 + \sigma_{\mathrm{C}}^2}\|\mathbf{H}\mathrm{diag}(\mathbf{F}_{\mathrm{RF}}\mathbf{D}_{\mathrm{R}}\mathbf{e}_{(1-\rho)N})\|_F^2). \tag{13}$$

Note that, $\|\mathrm{diag}(\mathbf{F}_{\mathrm{RF}}\mathbf{D}_{\mathrm{C}}\mathbf{e}_{\rho N})\|_F^2 = 2\rho\|\mathrm{diag}(\mathbf{F}_{\mathrm{RF}}\mathbf{D}_{\mathrm{C}})\|_F^2$, and $\|\mathrm{diag}(\mathbf{F}_{\mathrm{RF}}\mathbf{D}_{\mathrm{R}}\mathbf{e}_{(1-\rho)N})\|_F^2 = 2(1-\rho)\|\mathrm{diag}(\mathbf{F}_{\mathrm{RF}}\mathbf{D}_{\mathrm{C}})\|_F^2$ If we consider the approximation $\log(1+x)^a \approx \log(1+ax)$, then it can be shown that:

$$\begin{aligned}
&\log_2(1 + 2\rho\frac{1}{\sigma_n^2 + \sigma_{\mathrm{R}}^2}\|\mathbf{H}\boldsymbol{\Phi}_{\mathrm{C}}\|_F^2 \\
&\quad + \log_2(1 + 2(1-\rho)\frac{1}{\sigma_n^2 + \sigma_{\mathrm{C}}^2}\|\mathbf{H}\boldsymbol{\Phi}_{\mathrm{R}}\|_F^2) \\
&\approx 2\rho\log_2(1 + \frac{1}{\sigma_n^2 + \sigma_{\mathrm{R}}^2}\|\mathbf{H}\boldsymbol{\Phi}_{\mathrm{C}}\|_F^2) \\
&\quad + 2(1-\rho)\log_2(1 + \frac{1}{\sigma_n^2 + \sigma_{\mathrm{C}}^2}\|\mathbf{H}\boldsymbol{\Phi}_{\mathrm{R}}\|_F^2) \qquad (14) \\
&= I^{\mathrm{w}}, \qquad (15)
\end{aligned}$$

where $\boldsymbol{\Phi}_{\mathrm{C}} = \mathrm{diag}(\mathbf{F}_{\mathrm{RF}}\mathbf{D}_{\mathrm{C}})$ and $\boldsymbol{\Phi}_{\mathrm{R}} = \mathrm{diag}(\mathbf{F}_{\mathrm{RF}}\mathbf{D}_{\mathrm{R}})$.

References

[1] Cisco Annual Internet Report 2018-23 White Paper, Mar. 2020. [Available Online]

[2] Ericsson Mobility Report 2022, pp. 1-40, June 2022. [Available Online]

[3] B. Paul et al., "Survey of RF communications and sensing convergence research," *IEEE Access*, vol. 5, pp. 252-270, Dec. 2017.

[4] J. A. Zhang et al., "An overview of signal processing techniques for joint communication and radar sensing," *IEEE J. Sel. Topics Sig. Process.*, vol. 15, no. 6, pp. 1295-1315, Nov. 2021

[5] F. Liu et al., "Joint radar and communication designs: Applications, state-of-the-art, and the road Ahead," *IEEE Trans. Commun.*, vol. 68, no. 6, pp. 3834-3862, June 2020.

[6] Y. Cui et al., "Integrating sensing and communications for ubiquitous IoT: Applications, trends and challenges," *IEEE Network*, vol. 35, no. 5, pp. 158-167, Sept. 2021.

[7] A. Kaushik et al., "Towards 6G: Spectrally efficient joint radar and communication with RF selection, interference and hardware impairments," *IET Signal Processing*, vol. 16, no. 7, pp. 851-863, Sept. 2022.

[8] F. Liu, et al., "MU-MIMO communications with MIMO radar: From co-existence to joint transmission," *IEEE Trans. Wireless Commun.*, vol. 17, no. 4, pp. 2755-2770, Apr. 2018.

[9] K. V. Mishra et al., "Toward millimeter-wave joint radar communications: A signal processing perspective," *IEEE Sig. Process. Mag.*, vol. 36, no. 5, pp. 100-114, Sept. 2019.

[10] A. Kaushik et al., "Dynamic RF chain selection for energy efficient and low complexity hybrid beamforming in millimeter wave MIMO systems," *IEEE Trans. Green Commun. Netw.*, vol. 3, no. 4, pp. 886-900, Dec. 2019.

[11] A. Kaushik et al., "Joint bit allocation and hybrid beamforming optimization for energy efficient millimeter wave MIMO systems," *IEEE Trans. Green Commun. Netw.*, vol. 5, no. 1, pp. 119-132, Mar. 2021.

[12] E. Vlachos et al., "Radio-frequency chain selection for energy and spectral efficiency maximization in hybrid beamforming under hardware imperfections," *Proc. Royal Soc. A*, vol. 476, no. 2244, pp. 1-20, Dec. 2020.

[13] A. Kaushik et al., "Hardware efficient joint radar-communicati-ons with hybrid precoding and RF chain optimization," *IEEE Int. Conf. Commun. (ICC)*, pp. 1-6, June 2021.

[14] A. Kaushik et al., "Green joint radar-communications: RF selection with low resolution DACs and hybrid precoding," *IEEE Int. Conf. Commun. (ICC)*, pp. 1-6, May 2022.

[15] Z. Wang et al., "NOMA empowered integrated sensing and communication," *IEEE Commun. Letters*, vol. 26, no. 3, pp. 677-681, Mar. 2022.

[16] O. Dizdar et al., "Energy efficient dual-functional radar-communication: Rate splitting multiple access, low-resolution DACs, and RF chain selection," *IEEE Open J. Commun. Society*, vol. 3, pp. 986-1006, June 2022.

[17] A. Kaushik et al., "Waveform design for joint-radar communications with low complexity analog components," *IEEE Int. Symp. Joint Commun. Sensing (JC&S)*, pp. 1-5, Mar. 2022.

[18] S. Chen et al., "Pre-scaling and codebook design for joint radar and communication based on index modulation," *IEEE Global Commun. Conf.*, pp. 1-5, Dec. 2022.

[19] T. Huang et al., "MAJoRCom: A dual-function radar communication system using index modulation," *IEEE Trans. Sig. Process.*, vol. 68, pp. 3423-3438, May 2020.

[20] M. Di Renzo et al., "Communication models for reconfigurable intelligent surfaces: From surface electromagnetics to wireless networks optimization," *Proceedings of the IEEE*, vol. 110, no. 9, pp. 1164-1209, Sept. 2022.

[21] Q. Cheng et al., "Reconfigurable intelligent surfaces: Simplified-architecture transmitters—from theory to implementations," *Proceedings of the IEEE*, vol. 110, no. 9, pp. 1266-1289, Sept. 2022.

[22] W.Lu et al.,"Target detection in intelligent reflecting surface aided distributed MIMO radar systems," *IEEE Sensors Lett.*, vol. 5, no. 3, pp. 1–4, 2021.

[23] X. Wang, et al., "RIS-assisted spectrum sharing between MIMO radar and MU-MISO communication systems," *IEEE Wireless Commun. Lett.*, vol. 10, no. 3, pp. 594–598, 2021.

[24] Y. Li and A. Petropulu, "Dual-Function Radar-Communication System Aided by Intelligent Reflecting Surfaces," *arXiv:2204.04721*, Apr. 2022.

[25] W. Dinkelbach, "On nonlinear fractional programming", *Management Science*, vol. 13, no. 7, pp. 492-498, Mar. 1967.

[26] M. Grant and S. Boyd, "CVX: Matlab Software for Disciplined Convex Programming," Version 2.1, Mar. 2014.

[27] B. Tang and J. Li, "Spectrally constrained MIMO radar waveform design based on mutual information," IEEE Trans. Sig. Process., vol. 67, no. 3, pp. 821-834, 1 Feb. 2019.

[28] R. Xu et al., "Radar mutual information and communication channel capacity of integrated radar-communication system using MIMO," ICT Express, vol. 1, no. 3, pp. 102-105, Dec. 2015.

[29] Y. Yang and R. S. Blum, "MIMO radar waveform design based on mutual information and minimum mean-square error estimation," IEEE Trans. Aerospace Elect. Sys.,pp. 1-12, Jan. 2007.

[30] M. Bica et al., "Mutual information based radar waveform design for joint radar and cellular communication systems," IEEE Int. Conf. Acoustics, Speech Sig. Process. (ICASSP), pp. 3671-3675, Mar. 2016.

[31] D. Tse and P. Viswanath, "Fundamentals of Wireless Communication," Cambridge University Press, 2005.